JACS
JOURNAL OF THE AMERICAN CHEMICAL SOCIETY
Communication
pubs.acs.org/JACS

Topological Considerations for the Design of Molecular Donors with Multiple Absorbing Units

Lai Fan Lai,[†,‡] John A. Love,[†] Alexander Sharenko,[†] Jessica E. Coughlin,[†,∥] Vinay Gupta,[†,§] Sergei Tretiak,[∥] Thuc-Quyen Nguyen,[†,#] Wai-Yeung Wong,[‡] and Guillermo C. Bazan*[,†,⊥]

[†] Center for Polymers and Organic Solids, University of California, Santa Barbara, California 93106, United States

[‡] Institute of Molecular Functional Materials and Department of Chemistry and Institute of Advanced Materials, Hong Kong Baptist University, Waterloo Road, Hong Kong, P.R. China

[§] Organic and Hybrid Solar Cell Group, CSIR-National Physical Laboratory, Dr. K. S. Krishnan Marg, New Dehli, 110012, India

[∥] Theoretical Division and Center for Integrated Nanotechnologies, Los Alamos National Laboratory, Los Alamos, New Mexico 87545, United States

[⊥] Center of Excellence for Advanced Materials Research (CEAMR), King Abdulaziz University, Jeddah, Saudi Arabia

[#] Department of Chemistry, Faculty of Science, King Abdulaziz University, Jeddah, Saudi Arabia

Supporting Information

ABSTRACT: The molecule **AT1**, with two weakly conjugated chromophores, was designed, synthesized, and examined within the context of its film forming tendencies. While the addition of the second chromophore to the central core enables broadening of the absorption spectrum, this change is mostly apparent in films that are grown slowly. Grazing incidence X-ray scattering (GI-WAXS) analysis indicates that these spectral characteristics correspond to an increase in solid state ordering. This information, in combination with differential scanning calorimetry, suggests that the overall molecular shape provides a kinetic barrier to crystallization. As a result, one finds the absence of molecular order when **AT1** is combined with $PC_{71}BM$ in solution-cast blends. These findings highlight the importance of molecular topology when designing molecular components for solar cell devices.

Improvements in materials design, processing techniques, and device architectures have led to improvements in the power conversion efficiencies (PCE) of organic photovoltaic (OPV) devices.[1] Significant effort on blends comprised of narrow band gap polymer donors with fullerene acceptors in a bulk heterojunction (BHJ) architecture has led to PCE values on the order of 10%.[2] However, recent successes with molecular donors have led to renewed efforts to understand and optimize this class of materials because of their monodisperse nature and ease of purification relative to their polymeric counterparts.[3,4]

A molecular design that has garnered significant attention and led to high PCEs couples electron-rich donor (D) units and electron-deficient acceptor (A) units.[5,6] An example of this class of molecules is p-DTS$(FBTTh_2)_2$, shown in Figure 1, which has achieved a PCE of 9%.[7−9] As the internal quantum efficiency of molecular devices approaches unity, further advancements in molecular OPVs will likely require new strategies in molecular design. Such novel chemical architectures must either tune frontier energy levels to increase open circuit voltages (V_{OC}) or increase the number of absorbed photons and thereby the short-circuit current density (J_{SC}).

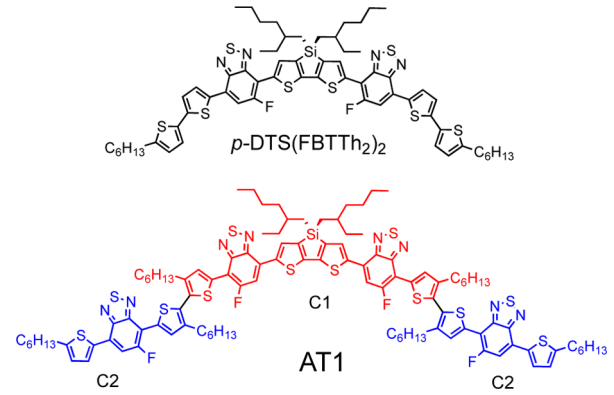

Figure 1. Compounds p-DTS$(FBTTh_2)_2$ and **AT1**.

Broad absorption may be achieved by coordinating different chromophores within a single molecule. This strategy has been successfully applied to oligothiophenes, with dye units as end caps.[10−12] In these examples, the dye units extend the conjugation length, and therefore adjust the electronic structure of the entire molecule. In this contribution we examine a different design strategy, which is based on integrating independent absorbing units at two ends of a symmetric core. Figure 1 shows the specific molecule **AT1**. The central chromophore **C1** (red) is linked on both sides with chromophore **C2** (blue). Although **C1** and the two **C2** units appear on paper to be conjugated, it was anticipated that they would absorb nearly independently as a result of the molecular topology, namely the twist in the conjugated backbone from steric interference between the hexyl side chains on the internal thiophene units. It also seemed reasonable that the internal

Received: February 18, 2014
Published: March 24, 2014

dx.doi.org/10.1021/ja501711m | J. Am. Chem. Soc. 2014, 136, 5591−5594

core of **AT1** would have the lowest energy transition and would determine the highest occupied molecular orbital (HOMO) energy level, due to the extended conjugation length and the presence of the electron-rich dithieno(3,2-*b*;2′,3′-*d*)silole (DTS) unit.

The synthesis of **AT1** is shown in Scheme S1, and the full synthetic and characterization details are provided in the Supporting Information (SI). Thin film cyclic voltammetry (CV) measurements show oxidation and reduction waves from which we estimate that the HOMO and lowest unoccupied molecular orbital (LUMO) energies are −5.29 and −3.14 eV, respectively, corresponding to a band gap of 2.1 eV (Figure S6). These data indicate that the frontier molecular orbitals of **AT1** are very similar to those of p-DTS(FBTTh$_2$)$_2$, suggesting that the levels are primarily determined by the **C1** core.[8]

Figure 2a shows that the absorption spectrum of **AT1** in chlorobenzene (CB) exhibits an onset of absorption (λ_{onset}) at

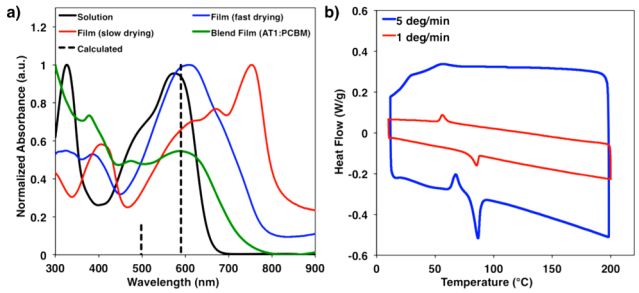

Figure 2. (a) Absorption spectra of **AT1** in solution and films at different drying rates. Dotted vertical lines represent calculated transitions. Also shown is the spectrum from a 60:40 **AT1**:PC$_{71}$BM blend film cast from CB and DIO. (b) DSC scans at two different speeds.

664 nm, corresponding to an optical band gap of 1.9 eV, and a broad absorption maximum (λ_{max}) at ∼575 nm. These features are similar to those of p-DTS(FBTTh$_2$)$_2$; however, in **AT1** a second absorption band is discernible as a shoulder at ∼475 nm. This second band is reasonably attributed to absorption of the **C2** chromophores, effectively broadening the range of absorption, compared with **C1** alone.

Density functional theory (DFT) calculations were employed using CAM-B3LYP/6-31G(d,p).[13,14] The minimum energy structure of **AT1** was calculated to have a dihedral twist angle of 57° between the two internal thiophenes; see Figure 3. Time-dependent DFT studies were completed using a dielectric similar to CB to determine excitation energies, and the calculated spectrum matches well with the experimentally

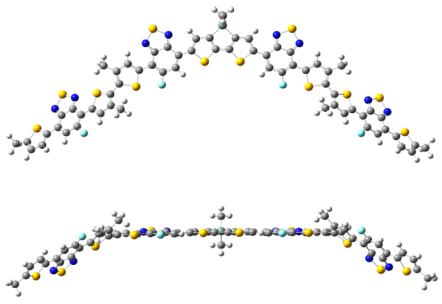

Figure 3. Top-down and side-on view of the lowest energy conformation of **AT1**.

determined spectrum (Figure S17).[15] Natural transition orbitals show that the transition around 480 nm is mainly from **C2** groups and the transition at 590 nm arises from **C1** almost exclusively (Table S3); see dashed lines in Figure 2a. Therefore, the twist angle of 57° effectively breaks electronic communication between **C1** and **C2**. The dependence of the absorption spectrum as a function of twist angle is provided in the SI.

Figure 2a also shows that the absorption of **AT1** films exhibits a large red shift compared to solution. The features are dependent on the evaporation rate of the CB. When spin-cast for 60 s and allowed to dry under nitrogen, λ_{max} = 620 nm. A broad, ill-defined shoulder peak appears at low energies that shifts λ_{onset} to 775 nm. A significantly different absorption is observed if the film is allowed to dry slowly in a closed Petri dish containing CB vapor. These conditions lead to shifts of λ_{max} to 760 nm and of λ_{onset} to 825 nm (band gap = ∼1.5 eV). The sharpness of these features suggests increased molecular order[16] relative to the as-cast samples and highlights the influence of processing history.

Differential scanning calorimetry (DSC) measurements of **AT1** were performed at different heating rates (Figure 2b and Figures S9−S10). At a rate of 5 °C/min, a cold crystallization is observed at 67 °C during the heating cycle, followed by a melting transition at 87 °C. No recrystallization peak is observed upon cooling. At the slower rate of 1 °C/min, a distinct melting temperature of 85 °C is observed with no indication of cold crystallization. However, upon cooling at the slower rate, the emergence of an exothermic peak at 56 °C was observed, identified as crystallization from the melt. Both the UV−visible absorption and DSC data therefore indicate that **AT1** has a substantial resistance to crystallization.

Grazing incidence wide-angle X-ray scattering (GIWAXS) was used to probe changes in **AT1** ordering; see Figure 4. The

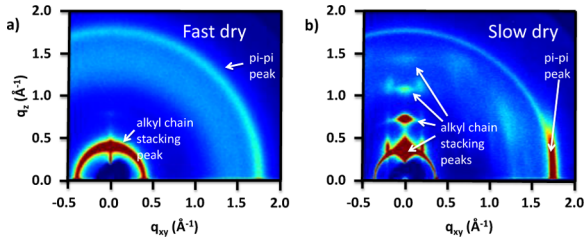

Figure 4. GIWAXS profiles of as-cast films of **AT1** spin coated from CB solution for 10 s: (a) slow drying; (b) fast drying.

GIWAXS pattern of the fast-dried film exhibits two isotropic peaks at approximately q = 0.37 and 1.77 Å^{-1}, corresponding to d-spacings of 17.0 and 3.5 Å, respectively. We assign the higher q reflection as the $\pi-\pi$ stacking peak and the lower q reflection as an "alkyl chain stacking peak", or arising from π-stacked units separated by alkyl side chains.[17−19] These spacings are consistent with structurally similar molecules[6,20,21] and common conjugated polymers.[22−24] The slow-dried film exhibits the same reflections, as well as additional reflections at q = 0.74, 1.09, and 1.46 Å^{-1}. These additional reflections are attributed to higher order alkyl chain stacking peaks. The $\pi-\pi$ stacking peak in the slow-dried film is highly anisotropic, appearing primarily in the in-plane direction. This suggests **AT1** preferentially π-stacks in the plane of the substrate, though a more specific understanding of molecular orientation is not possible at this stage, as attempts to grow a suitable single crystal were unsuccessful. The presence of higher order

dx.doi.org/10.1021/ja501711m | J. Am. Chem. Soc. 2014, 136, 5591−5594

reflections and a preferred orientation of crystallites indicate that **AT1** films are able to achieve a greater degree of order when evolved more slowly.

Atomic force microscopy reveals that slow versus fast drying leads to considerably different surface topographic features; see Figure S13. Specifically, coarser and blockier features are observed for the slow dried film, compared to a fiber-like morphology when the film dries more quickly.

Charge transport was examined by using a hole-only diode structure in which a film of **AT1** was sandwiched between an ITO/poly(3,4-ethylenedioxythiophene)poly(styrene sulfonate) (PEDOT:PSS) bottom electrode and an evaporated Au top contact. Devices containing slow dried films were all electrically shorted, presumably because of the inhomogeneous surface features. Diodes fabricated with the quickly dried films were fit with the space charge limited current model described by the Mott–Gurney law (SI) to give a hole mobility of $\mu_p = 2.5 \times 10^{-4}$ cm^2/(Vs), comparable with other BHJ donor materials.[25,26]

Using solution casting conditions which have been successful for structurally similar molecules[8,27] (35 mg/mL chlorobenzene, 50:50 **AT1**:$PC_{71}BM$), the initial examination of solar cells utilized the device architecture of glass/ITO(∼150 nm)/PEDOT:PSS(∼35 nm)/BHJ(∼80 nm)/Al(∼100 nm). Blends were cast from pure solvent, as well as with small amounts of the solvent additive diiodooctane (DIO); see Figure S11. As-cast from CB, **AT1**:$PC_{71}BM$ solar cells show negligible performance (PCE = 0.3%, V_{OC} = 0.59 V, J_{SC} = 1.78 mA/cm^2, *FF* = 26%). Addition of 0.4% DIO by volume to the casting solution enhances the PCE to 1.3% (V_{OC} = 0.75 V, J_{SC} = 6.39 mA/cm^2, *FF* = 27%). This increase in V_{OC} begins to approach what would be expected empirically based on the energy levels of **AT1**.[8]

Crystallization of the donor within the BHJ blend has proven paramount to providing effective molecular OPVs.[21,27,28] We therefore examined the order within any **AT1** phase in the BHJ blend films first by examining the absorption profiles of **AT1**:$PC_{71}BM$ films obtained from a number of conditions (Figure S11). Despite different solvent, additive, and thermal annealing conditions, the absorption of the blends exhibit no evidence of the vibronic structure related to **AT1** crystallization; see the green trace in Figure 2a for a representative example. GIWAXS spectra for blend films with and without DIO, provided in Figure S12, appear almost identical. Although there is some scattering in the region where one would expect alkyl chain stacking reflections from **AT1**, there are no clear features. There is also no apparent indication of any $\pi-\pi$ stacking peak. It is evident that the incorporation of $PC_{71}BM$ prevents **AT1** from overcoming the kinetic barrier to crystallization resulting in a very poorly organized BHJ blend. Additionally, blends of **AT1** with two other common acceptor molecules, a perylenediimide and vinazene derivative, showed no evidence of vibronic structure in the absorption traces either (Figure S14) indicating that difficulties in crystallization are specific to the structure of the donor material.

In conclusion, **AT1** is a single molecule with nearly independent chromophores. The key structural feature is the breakup of delocalization between the **C1** and **C2** absorbing units via the nonplanar relationship between the two internal thiophene heterocycles. While this feature achieves the desirable objective within the context of the molecule's electronic structure, as inferred from absorption characteristics and DFT analysis, it provides **AT1** with an overall nonplanar topology; see Figure 3. This "awkward" structure is reminiscent of spiro-type and tetrahedral multichromophore systems that are resistant to crystallization and often provide amorphous thin films.[29,30] A combination of GIWAXS and absorption spectroscopy shows that it is possible to find growth conditions through slow solvent evaporation that yield ordered films of pure **AT1**. However, the introduction of $PC_{71}BM$ exacerbates the kinetic barriers for **AT1** crystallization from solution. This absence of crystallization likely impedes achieving the BHJ morphology necessary for achieving high PCE. Looking forward, the work highlights the need for developing new processing strategies that allow different film growth profiles of BHJ blends and for design strategies that allow incorporation of multiple absorbing units within a planar molecular topology.

■ ASSOCIATED CONTENT

Supporting Information

Full experimental information, solar cell fabrication, thin film characterization, and full computational report are available. This material is available free of charge via the Internet at http://pubs.acs.org.

■ AUTHOR INFORMATION

Corresponding Author

*E-mail: bazan@chem.ucsb.edu.

Notes

The authors declare no competing financial interest.

■ ACKNOWLEDGMENTS

Financial support for the synthesis of the molecules was provided by the Office of Naval Research (N00014-11-1-0284). V.G. was supported by the Indo-US Science and Technology Forum (IUSSTF), Award No. Indo-US Research Fellowship/2012-2013/26-2012. A.S. would like to acknowledge support from a National Science Foundation Graduate Research Fellowship. J.L. is supported by the Center for Energy Efficient Materials, an Energy Frontier Research Center funded by the Office of Basic Energy Sciences of the U.S. Department of Energy. W.-Y.W. thanks the University Grants Committee of HKSAR, China (Project No. [AoE/P-03/08]), Hong Kong Research Grants Council (HKBU202410) and Hong Kong Baptist University for financial support. Portions of this research were carried out at the Stanford Synchrotron Radiation Light Source user facility operated by Stanford University on behalf of the U.S. Department of Energy, Office of Basic Energy Sciences. We also acknowledge support of the Los Alamos National Laboratory (LANL) Directed Research and Development program. LANL is operated by Los Alamos National Security, LLC, for the National Nuclear Security Administration of the U.S. Department of Energy under Contract DE-AC52-06NA25396.

■ REFERENCES

(1) Brabec, C.; Scherf, U.; Dyakonov, V. *Organic Photovoltaics: Materials, Device physics, and Manufacturing Technologies*; Wiley: 2011.

(2) You, J.; Dou, L.; Yoshimura, K.; Kato, T.; Ohya, K.; Moriarty, T.; Emery, K.; Chen, C.-C.; Gao, J.; Li, G.; Yang, Y. *Nat. Commun.* **2013**, *4*, 1446.

(3) Roncali, J. *Acc. Chem. Res.* **2009**, *42*, 1719.

(4) Lin, Y.; Li, Y.; Zhan, X. *Chem. Soc. Rev.* **2012**, *41*, 4245.

(5) Li, Y.; Guo, Q.; Li, Z.; Pei, J.; Tian, W. *Energy Environ. Sci.* **2010**, *3*, 1427.

(6) Welch, G. C.; Perez, L. A.; Hoven, C. V.; Zhang, Y.; Dang, X.-D.; Sharenko, A.; Toney, M. F.; Kramer, E. J.; Nguyen, T.-Q.; Bazan, G. C. *J. Mater. Chem.* **2011**, *21*, 12700.
(7) Kyaw, A. K. K.; Wang, D. H.; Gupta, V.; Zhang, J.; Chand, S.; Bazan, G. C.; Heeger, A. J. *Adv. Mater.* **2013**, *25*, 2397.
(8) van der Poll, T. S.; Love, J. A.; Nguyen, T.-Q.; Bazan, G. C. *Adv. Mater.* **2012**, *24*, 3646.
(9) Gupta, V.; Kyaw, A. K. K.; Wang, D. H.; Chand, S.; Bazan, G. C.; Heeger, A. J. *Sci. Rep.* **2013**, *3*, 1965.
(10) Li, Z.; He, G.; Wan, X.; Liu, Y.; Zhou, J.; Long, G.; Zuo, Y.; Zhang, M.; Chen, Y. *Adv. Energy Mater.* **2012**, *2*, 74.
(11) Zhou, J.; Wan, X.; Liu, Y.; Zuo, Y.; Li, Z.; He, G.; Long, G.; Ni, W.; Li, C.; Su, X.; Chen, Y. *J. Am. Chem. Soc.* **2012**, *134*, 16345.
(12) Liu, Y.; Chen, C.-C.; Hong, Z.; Gao, J.; Yang, Y.; Zhou, H.; Dou, L.; Li, G.; Yang, Y. *Sci. Rep.* **2013**, *3*, 3356.
(13) Yanai, T.; Tew, D. P.; Handy, N. C. *Chem. Phys. Lett.* **2004**, *393*, 51.
(14) Zhugayevych, A.; Postupna, O.; Bakus, I.; Ronald, C.; Welch, G. C.; Bazan, G. C.; Tretiak, S. *J. Phys. Chem. C* **2013**, *117*, 4920.
(15) Takano, Y.; Houk, K. N. *J. Chem. Theory Comput.* **2005**, *1*, 70.
(16) Ostroverkhova, O.; Shcherbyna, S.; Cooke, D. G.; Egerton, R. F.; Hegmann, F. A.; Tykwinski, R. R.; Parkin, S. R.; Anthony, J. E. *J. Appl. Phys.* **2005**, *98*, 033701.
(17) Baker, J. L.; Jimison, L. H.; Mannsfeld, S.; Volkman, S.; Yin, S.; Subramanian, V.; Salleo, A.; Alivisatos, A. P.; Toney, M. F. *Langmuir* **2010**, *26*, 9146.
(18) Rogers, J. T.; Schmidt, K.; Toney, M. F.; Kramer, E. J.; Bazan, G. C. *Adv. Mater.* **2011**, *23*, 2284.
(19) Du, C.; Li, W.; Duan, Y.; Li, C.; Dong, H.; Zhu, J.; Hu, W.; Bo, Z. *Polym. Chem.* **2013**, *4*, 2773.
(20) Love, J. A.; Nagao, I.; Huang, Y.; Kuik, M.; Gupta, V.; Takacs, C. J.; Coughlin, J. E.; Qi, L.; van der Poll, T. S.; Kramer, E. J.; Heeger, A. J.; Nguyen, T.-Q.; Bazan, G. C. *J. Am. Chem. Soc.* **2014**, *136*, 3597.
(21) Love, J. A.; Proctor, C. M.; Liu, J.; Takacs, C. J.; Sharenko, A.; van der Poll, T. S.; Heeger, A. J.; Bazan, G. C.; Nguyen, T.-Q. *Adv. Funct. Mater.* **2013**, *23*, 5019.
(22) Chu, C.-W.; Yang, H.; Hou, W.-J.; Huang, J.; Li, G.; Yang, Y. *Appl. Phys. Lett.* **2008**, *92*, 103306.
(23) Ma, W.; Yang, C.; Gong, X.; Lee, K.; Heeger, A. J. *Adv. Funct. Mater.* **2005**, *15*, 1617.
(24) Chabinyc, M. L.; Toney, M. F.; Kline, R. J.; McCulloch, I.; Heeney, M. *J. Am. Chem. Soc.* **2007**, *129*, 3226.
(25) Walker, B.; Kim, C.; Nguyen, T.-Q. *Chem. Mater.* **2011**, *23*, 470.
(26) Craciun, N. I.; Wildeman, J.; Blom, P. W. M. *Phys. Rev. Lett.* **2008**, *100*, 056601.
(27) Sun, Y.; Welch, G. C.; Leong, W. L.; Takacs, C. J.; Bazan, G. C.; Heeger, A. J. *Nat. Mater.* **2012**, *11*, 44.
(28) Takacs, C. J.; Sun, Y.; Welch, G. C.; Perez, L. A.; Liu, X.; Wen, W.; Bazan, G. C.; Heeger, A. J. *J. Am. Chem. Soc.* **2012**, *134*, 16597.
(29) Kanibolotsky, A. L.; Perepichka, I. F.; Skabara, P. J. *Chem. Soc. Rev.* **2010**, *39*, 2695.
(30) Skabara, P. J.; Arlin, J.-B.; Geerts, Y. H. *Adv. Mater.* **2013**, *25*, 1948.